Magnetically Separable CoFe₂O₄/CuO Photocatalyst for Degradation of Methylene Blue under Visible Light

Bahareh Jozv Khatibzdeh[a], Narjes Keramati[b,*] , Mohsen Mehdipour Ghazi[a]

[a]*Department Chemical, Petroleum and Gas Engineering, Semnan University, Semnan, Iran.*
[b]*Faculty of New Science & Technology, Department of Nanotechnology, Semnan University, Semnan, Iran.*

Abstract

Currently, the need for more efficient materials that work in the visible light spectrum for water treatment has been increasing. A CoFe₂O₄/CuO nanocomposite was successfully synthesized by co-precipitation method. The obtained nanocomposite was characterized by XRD, DRS, FT-IR and FESEM. X-ray diffraction data showed that the obtained nanoparticle was composed of CoFe₂O₄ and CuO with average crystal size of 36nm. The optical absorption spectrum of the CuO/CoFe₂O₄ nanocomposite displayed a band gap of 2.75 eV. The materials showed photocatalytic activity due to the presence of Cu, associated with the magnetic activity of CoFe₂O₄, which is useful for the separation and recovery of the photocatalyst after use in an oxidative process. Photocatalytic activity was studied by degradation of methylene blue under visible light. Compared with pure CuO, the CoFe₂O₄/CuO nanocomposite exhibited improved photodegradation performance (about five more time). To optimize process and obtain a mathematical model, CCD (with three factors at five levels) was used. The optimal conditions were determined where the amount of photocatalyst= 1 g/L, irradiation time= 140 min and the concentration of MB= 15 ppm with optimum degradation efficiency as 84.98%. The synthesized CoFe₂O₄/CuO nanocomposite can be potentially used as a visible-light responsive magnetically separable photocatalyst.

Keywords: Photocatalyst, CoFe₂O₄/CuO, Methylene Blue, Visible Light.

1. Introduction

Metal-oxide nanoparticles have been extensively utilized in various applications [1], including advanced oxidation processes (AOPs), due to their interesting physicochemical properties [2-5]. Apart from the widely used photocatalysts such as TiO₂ and ZnO, p-type semiconductor CuO has been employed as an effective photocatalyst due to its high photochemical stability [6, 7]. The recovery of nano photocatalysts from a heterogeneous suspension in general is one of the difficulties associated with water and wastewater purification. Magnetic nano photocatalysts can be easily separated from the heterogeneous suspension by application of a magnetic field [8]. Iron and cobalt oxides

---

* **.Corresponding Author:** Assistant Professor of Chemical Engineering-Nanotechnolgoy, Semnan University, Faculty of New Sciences and Technollogies, Department of Nanotechnology, Semnan, Iran. E-mail Address: narjeskeramati@semnan.ac.ir

exhibit excellent magnetic and photocatalytic properties. The synthesis of nano-sized ferrite magnetic materials have been extensively studied because of their potential applications in high-density magnetic recording, microwave devices, drug delivery applications, etc. [8, 9]. Among these, $CoFe_2O_4$ has long been of intensive importance in the fundamental sciences and technological applications in various fields such as catalysis. The applications of $CoFe_2O_4$ are strongly influenced by its magnetic properties.

Various synthetic approaches have been employed to prepare cobalt ferrite-copper oxide nano particles, such as sol-gel, chemical co-precipitation, forced hydrolysis in a polyol medium, synthesis in oil-in-water micelles, and in reverse micelles, or thermal decomposition of a mixed Co^{2+}–Fe^{3+} oleate complex [10-12]. The co-precipitation process is an efficient method to prepare ultra-fine particles dispersed in different matrices [13].

The aim of this study is to obtain a magnetically separable photocatalyst, which is stable, well dispersed, and easy to prepare. In this research, efficacy study of $CoFe_2O_4$/CuO as a photocatalyst for degradation of methylene blue (MB) in the presence of visible light is investigated. The heterogeneous photocatalyst can be separated and collected with a magnet from an aqueous suspension. This is a profound advantage when the catalyst used in practice, because separating ultra-fine catalyst is a serious problem, which impedes the application of CuO photocatalyst at industrial scale. Furthermore, this heterogeneous photocatalyst have considerable activity in visible light region.

2. Experimental procedure

2. 1 Materials and method

All chemical reagents were obtained from Merck Company and were used without further purification. Distilled deionized water were used in all experiments. In a typical run, 200 ml Co $(NO_3)_2.6H_2O$ (0.5 M) and Fe $(NO_3)_3.9H_2O$ (1.0M) mixture solution was dropped

3. Results and Discussion

3.1. Characterization

The X-ray diffraction patterns for as-synthesized CuO/$CoFe_2O_4$ and as-received CuO nanoparticles are

into a 100 ml NaOH solution until pH 12. During the precipitation process, the reaction solution was vigorously stirred and 0.1 M NaOH solution was added to keep pH value as the initial stage. Then 1 gr CuO was added. The precipitate was aged for 3 hours at 90 ºC. It was then filtered out and washed with distilled water several times. Then, the precipitate was dried at 110 ºC for 12h. The powders was then calcined at 400 ºC for 5 hours. The prepared photocatalysts were characterized via various analytical methods. The crystal structures were characterized via X-ray diffraction (XRD) analysis (Bruker/D8) with Cu-Kα radiation (λ= 0.1546 nm). The UV–vis absorption spectra were recorded using a UV–vis spectrophotometer (UV-1650PC, Shimadzu). The Diffusive reflectance Spectra (DRS) of the samples were recorded by an UV–Vis Spectrophometer (Avantes, Avaspec 2048 TEC). A Fourier transform infrared Spectrometer (FT-IR Shimadzu, 8400 S) was used to determine the functional groups of the photocatalysts. The structures of the sample were observed with a scanning electron microscope (TESCAN).

The photo degradation experiment was performed in an aqueous solution containing methylene blue ($C_{16}H_{18}N_3SCl$). A photo reactor made of Pyrex glass was filled with 300 ml aqueous solution of MB at selected concentration. The catalyst loading amount was adjusted. The catalytic reaction was conducted at room temperature. Two visible lamps of 60W (Philips) was used. Before irradiation, the adsorption equilibrium of dye was attained in the dark during 30 min. Then the solution was put under irradiation and the reaction was monitored by UV–Vis spectrophotometer at maximum absorbance wavelength of MB (λ = 664 nm).

shown in Fig. 1. As shown, the discernible peaks can be indexed to (220), (311), (422), (511) and (440)

planes of a cubic structure $CoFe_2O_4$, which are characteristics for in cubic spinel-type and match well with standard data (JCPDS card no. 22-1086). Also, two reflection at $2\theta=35.3$ (002) and $2\theta=39$ (111) were observed in the diffraction patterns, and are ascribed to

the formation of the CuO monoclinic crystal phase. The crystallite size for the most intense peak was calculated from the XRD data using the Deby-Scherrer equation about 36 nm.
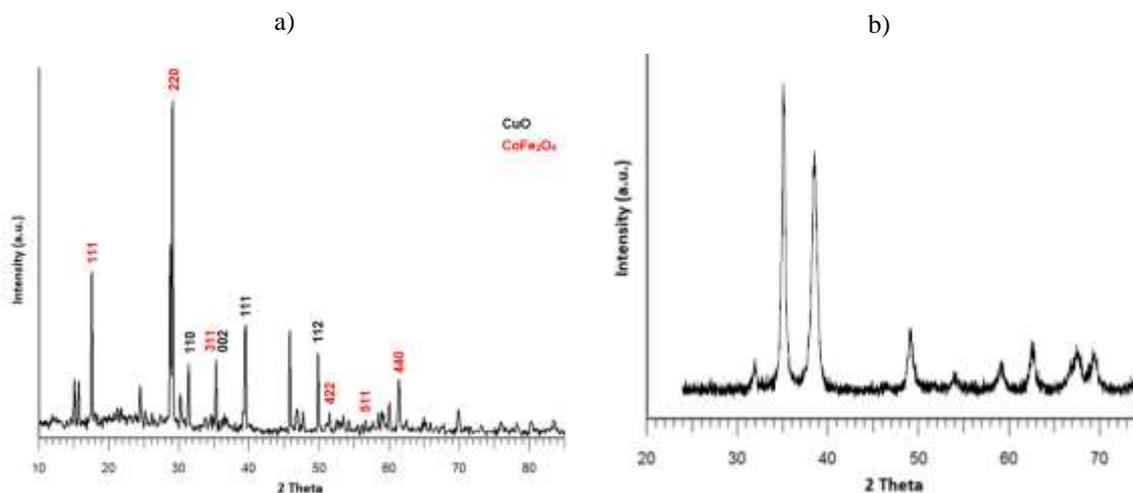
a)   b)

Fig. 1 XRD pattern of a) as-synthesized $CuO/CoFe_2O_4$ nanoparticle, b) as-received CuO nanoparticle.

Fig. 2 shows the adsorption bands of cobalt ferrite in 585 cm^{-1}, which was related to the vibration of metallic ions (Fe-O and Co-O) in the spinel structure [14]. A broad peak around 3168 cm^{-1} is attributed to stretching

O-H group absorbed on the surface of the nanoparticles. The absorption band of 525 cm^{-1} indicates the formation of the Cu-O bond [15].
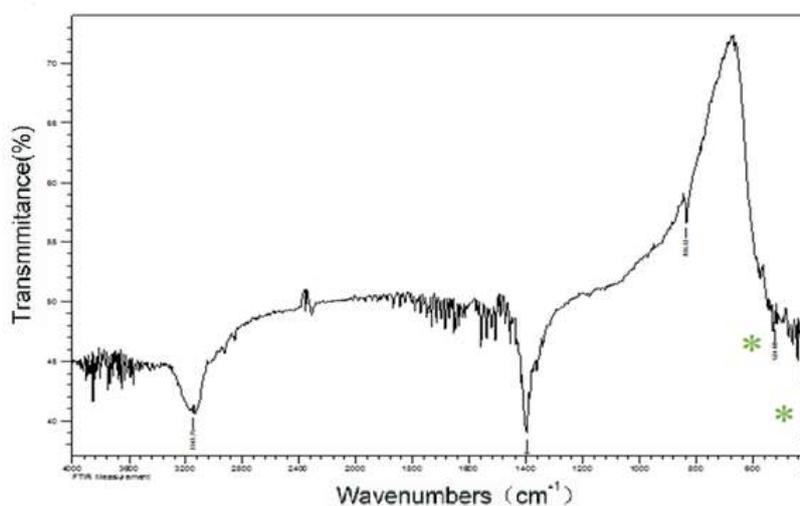

Fig. 2. FT-IR analysis of as-synthesized $CuO/CoFe_2O_4$ nanoparticle.

Fig. 3 gives the UV–vis diffuse reflectance spectra of cobalt ferrite – copper oxide composite. It can be clearly seen that the intensity of absorbance of composite increases significantly in the range of 200–

900 nm, which indicates that the band edge absorption has been broadened to visible light region. This composition can introduce a new impurity level to the conduction band of CuO and the electrons can be

promoted from the valence band to these impurity levels, resulting in a narrowing of band gap. This fact indicates that there are more photo generated electrons and holes which can be introduced to participate in the photocatalytic reactions. This result is advantageous to broaden the response region of cobalt ferrite – copper oxide composite to visible light and to use solar light as light source in the degradation of dye wastewater. The band gap energy can be roughly calculated by the $E_g = 1240/\lambda_{onset}$ formula, where λ_{onset} is the absorption onset wavelength [16]. The optical absorption spectrum of the $CuO/CoFe_2O_4$ nanocomposite displayed a band gap of 2.75 eV, which made it a suitable candidate for application in photocatalytic degradation of organic pollutants.
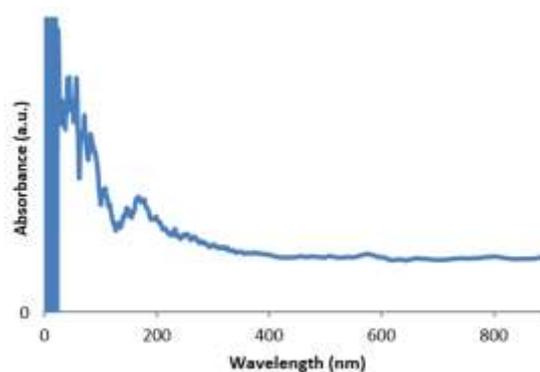

Fig. 3. DRS of as-synthesized $CuO/CoFe_2O_4$.

Fig. 4a shows the image Field emission scanning electron microscopy associated with the cobalt ferrite-copper oxide. The images represent the formation of a cobalt ferrite-copper oxide nano photocatalyst in a dimension of 42.76 nm with irregular spherical morphology. Fig. 4b shows the image of scanning electron microscopy of as-received CuO nanoparticles.
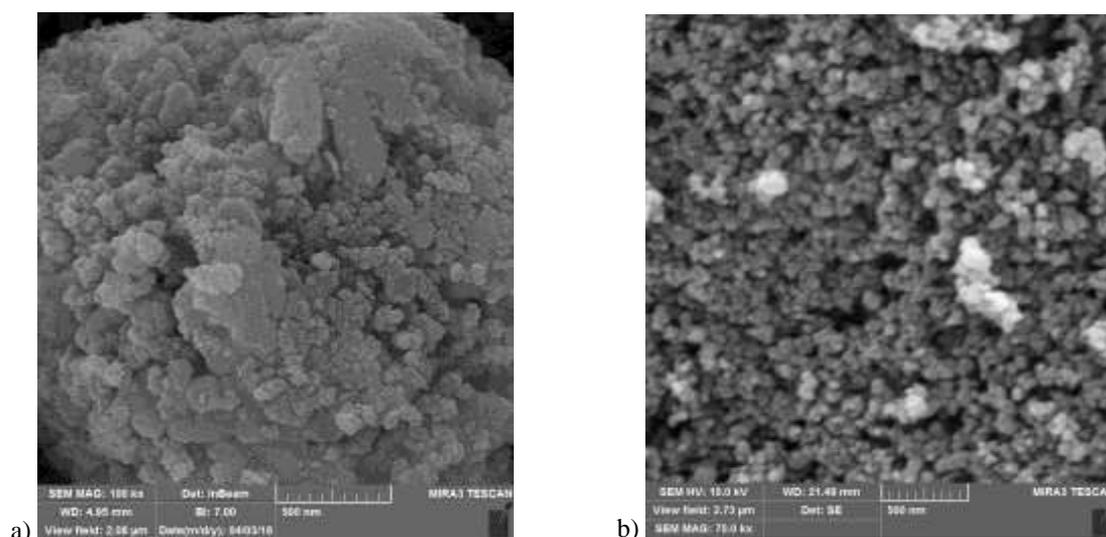

Fig. 4. Fe-SEM image of a) as-synthesized $CuO/CoFe_2O_4$, b) as-received CuO nanoparticle.

3.2. Photocatalytic Degradation of MB

To evaluate the photocatalytic activity of cobalt ferrite – copper oxide nanoparticle, the degradation of MB was investigated. For comparison, the MB degradation over CuO was also carried out under identical conditions. The decolorizing efficiency of MB solution by using cobalt ferrite – copper oxide was five times greater than copper oxide. This result obviously indicates that the presence of $CoFe_2O_4$ effectively enhances the photocatalytic activity of CuO under visible light. Furthermore, due to magnetic properties of $CoFe_2O_4$, catalyst separation from solution became easier (Fig. 5).

Fig. 5. magnetic properties of as-synthesized CuO/CoFe$_2$O$_4$ nanoparticle.

The three selected experimental parameters were optimized using RSM considering them as independent variables and degradation efficiency as response variable. The ranges and levels of independent variables are shown in Table 1. Multivariate regression analysis and optimization process were performed using Design Expert software version 8.0.4.1.

The CCD experiments matrix and experimental results are presented in Table 2. According to run number of 4,6,10,16, 19 and 20, degradation with as-synthesiez photocatalyst has repeatable. In the process of repeatability, the photocatalyst was reused in the next run without any changes. This experimental data was fitted using response surface analysis based on Eq (1) in terms of actual factors to predict degradation efficiency:

$$D = -03.27396 + 270.03209A + 25.38705B + 5.27639C - 6.15000AB - 1.66875AC - 0.17813BC \quad (1)$$

Table 1. Values of chosen variables for CCD.

variable	-α	-1	0	+1	+α
CuO/CoFe$_2$O$_4$ Concentration (A) (gL^{-1})	0.83	1	1.25	1.50	1.67
MB Concentration (B) (mgL^{-1})	13.30	15	17.50	20	21.70
Irridiation time (C) (min)	86.36	100	120	140	153.64

Table 2. Experimental design matrix and the value of responses based on experiment runs.

Run	Independent variables			Degradation efficiency (%)
	A	B	C	Experimental
1	0.83	17.5	120	67.5
2	1.25	17.5	86.36	51.75
3	1.25	17.5	153.64	52.5
4	1.25	17.5	120	52.5
5	1	20	140	58.5
6	1.25	17.5	120	54.75
7	1	15	140	87
8	1.5	15	100	52.5
9	1.5	15	140	57.75
10	1.25	17.5	120	54
11	1.25	13.3	120	69.75
12	1	20	100	55.5
13	1.5	20	100	44.25
14	1.5	20	140	15
15	1	15	100	47.25
16	1.25	17.5	120	53.25
17	1.25	21.7	120	37.5
18	1.67	17.5	120	37.5
19	1.25	17.5	120	53.25
20	1.25	17.5	120	54

Table 3. Analysis of variance results.

pValue	F- Value	Mean Square	df	Sum of Squares	variables
<0.0001	249.60	619.08	6	3714.46	Model
<0.0001	492.84	1222.36	1	1222.36	A:catalyst
<0.0001	464.90	1153.06	1	1153.06	B:MB
0.0044	11.82	29.32	1	29.32	C:time
<0.0001	47.65	118.20	1	118.20	AB
<0.0001	224.55	556.95	1	556.95	AC
<0.0001	255.85	634.57	1	634.57	BC
		2.48	13	32.24	Residual
0.0333	5.89	3.64	8	29.15	Lack of Fit
		0.62	5	3.09	Pure Error

Model sufficiency was investigated via analysis of variance (ANOVA-Table 3). Lack of fit (LoF) which compares residual error with pure error was also checked and shown to be not significant in comparison with pure error. The model regression coefficient (R^2 = 0.9914) shows that 99.14% of variability in degradation can be explained by the predicted model. Moreover, adjusted determination coefficient (R^2 adj.) is equal to 0.9874, which is high enough to prove significance of model.

Finally, estimated P-values should be examined to confirm the adequacy of the 2FI model. If P-value is smaller than 0.05, the model terms will be significant [16-18]. As shown in Table 1, variables of catalyst concentration, pollutant dosage, time of intensity were highly significant (P-values of <0.0001, <0.0001, 0.0044 and <0.0001, respectively). Normal probability plot of residuals was also used to evaluate the validity of the model. Fig. 6 shows that residuals (differences between observed and predicted responses) formed an approximately straight line and followed a normal distribution.
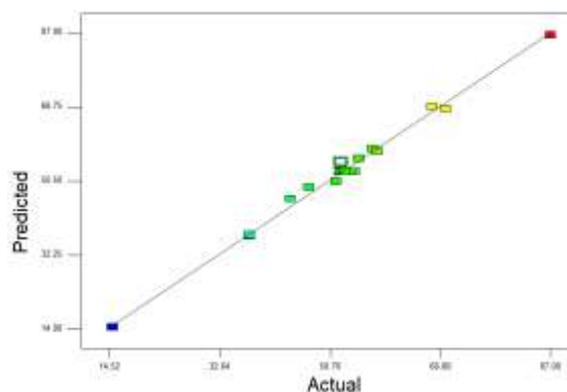

Fig. 6. Normal probability plot of residuals.

3.2.1. Effect of photocatalyst dosage

The effect of catalyst loading on the pollutant degradation was investigated in the range of 1–1.5 g/L. As shown in Fig. 7, degradation efficiency was developed with decrease of catalyst concentration. By increasing the amount of photocatalyst, the number of active sites on the surface of the catalyst increases and leads to increased radical hydroxyl and superoxide. As a result, photocatalytic activity and pollutant degradation efficiency has increased. But more catalyst loading may result in degradation efficiency reduction. This phenomenon was related to increased scattering and turbidity effects, which does not allow the penetration of light into all available surface of particles. On the other hand, the agglomeration of particles results in the decrease of activated reaction sites [17-19].

3.2.2. Effect of Methylene blue concentration

According to Fig. 7, degradation efficiency was decreased with the increase of initial MB concentration which is attributed to some reasons. When initial pollutant concentration increases, more particles of MB are adsorbed on the photocatalyst

active surfaces. In this case, reactive species quantity (.OH and .O_2^-) does not change because catalyst dosage, light intensity and reaction time are kept constant. Therefore present reactive radicals are not enough for high MB concentrations. In addition, production of intermediates may occur when substrate concentration increases, which leads to diffuse in photocatalyst surface and deactivates reaction sites [17-19].

3.2.3. Effect of irradiation time

As illustrated in Fig. 8, time is an important parameter which directly affects degradation efficiency. With irradiation time increment from 100 min to 140 min, photocatalyst particles will have more opportunity to participate in photocatalytic reactions.

3.2.4. Determination of optimum condition

With respect to efficiency and cost, desired goals were defined as maximum degradation and minimum catalyst loading, respectively. The optimized

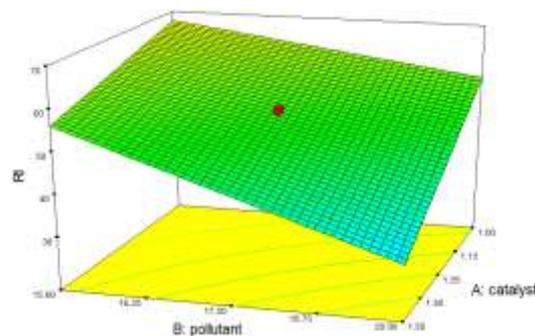degradation efficiency and operating conditions from model are presented in Table 4.

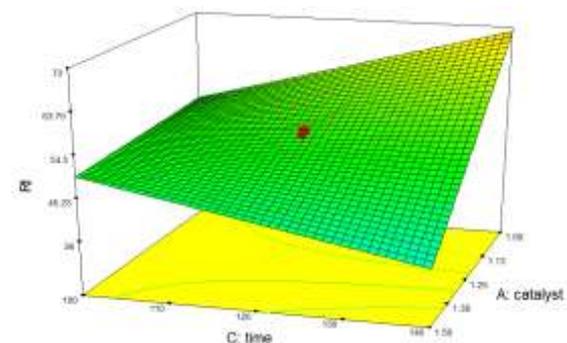**Fig. 7.** Effect of catalyst dosage and pollutant concentration on degradation efficiency.

Fig. 8. Effect of catalyst dosage and irradiation time on degradation efficiency.

Table 4. Optimized degradation efficiency and operating conditions.

experimental degradation percent	Predicted degradation percent	Desirability	Time (min)	catalyst loading (g/lit)	initial MB concentration (ppm)
84.98	86.31	0.995	140	1	15

4. Conclusion

In summary, cobalt ferrite- copper oxide composite were successfully synthesized through co – precipitation method. The presence of $CoFe_2O_4$ broadened the response region of CuO to visible light. The obtained $CoFe_2O_4$/CuO nanocomposite was characterized by X-ray diffraction for phase composition and crystallinity. The composite exhibited higher photocatalytic activity in comparison with CuO. The incorporation of magnetic $CoFe_2O_4$ provided a way to solve the embarrassments in practical applications, separation and recovery of CuO. The combination of the photocatalysis properties of CuO, and magnetic property of $CoFe_2O_4$ particles endowed this material with a bright perspective in

purification of polluted wastewater. Furthermore, these composite can be separated and collected with a magnet for reuse in photocatalytic process and effectively avoid the secondary pollution of the treated water.

References

[1] P. Sathishkumar, R. Viswanathan Mangalaraja, S. Anandan, M. Ashokkumar, *Chem. Eng. J*, **220** (2013) 302.

[2] R. Mohammadzadeh Kakhki, F. Entezari, A. Nik Nahad, *J. Of Applied Chemistry*, **15** (1399) 113, in Persian.

[3] K. Anil Isai, V. Shankar Shrivastava, *Iran. J. Catal*, **9**(3) (2019) 259.

[4] S. Dianat, Iran. J. Catal, 8(2) (2018) 121.

[5] A.R. Amani Ghadim, Kh. Lotfi Hayaee, M.S. Seyed Deraji, *J. Of Applied Chemistry*, **12** (1396) 55, in Persian.

[6] M. Ranjeh, F. Beshkar, O. Amiri, M. Salavati-Niasari, H. Moayedi, *J. Alloy Compd*, **815** (2020) 152451

[7] H. Salari, M. Sadeghinia, *J. Photochem. Photobiol. A*, **376** (2019) 279.

[8] S. Hashemi-Uderji, M. Abdollahi-Alibeik, R. Ranjbar-Karimi, *Iran. J. Catal*, **8**(4) (2018) 311.

[9] Y. Wang, D. Su, A. Ung, J.H. Ahn and G. Wang, *Nanotechnology*, **23** (2012) 402.

[10] V. Kumar Gupta, T. Eren, N. Atar, M. Lütfi Yola, C. Parlak, H. Karimi-Maleh, *J. Mol. Liq*, **208** (2015) 122.

[11] J. Huang, H.X. Jing, N. Li, L.X. Li, W. Zh. Jiao, *J. Solid State Chem*, **271** (2019) 103.

[12] H. Gong, W. Chu, *J. Hazard. Mater*, **314** (2016) 197.

[13] Q. Ma, L. Ch. Nengzi, X. Zhang, Zh. Zhao, X. Cheng, *Sep. Purif. Technol*, **233** (2020) 115978.

[14] A. Pui, D. Gherca, G. Carja, Dig. *J. Nanomater. Bios*, **6**(4) (2011) 1783.

[15] V. Vellora Th. Padil, M. Cernik, *Int. J. Nanomedicine*, **8** (2013) 889.

[16] M. Sabonian, K. Mahanpoor, *Iran. J. Catal*, **9**(3) (2019) 201.

[17] N. Keramati, N. Fallah, B. Nasernejad, *Desalin. Water Treat*, **57** (2016) 19239.

[18] N. Keramati, B. Nasernejad, N. Fallah, *J. Disper. Sci. Technol*, **35** (2014) 1543.

[19] F. Saadati, N. Keramati, M. Mehdipour Ghazi, *Crit. Rev. Env. Sci. Technol,* **46** (2016) 757.